Journal of the Southeastern Association for Research in Astronomy, **3**, 2-5, 2010 March 1

THE DOPPLER FOOTPRINT OF COLLIDING BINARY WINDS IN EMISSION LINE PROFILE SHAPES

C. S. Price[1] and Richard Ignace
Department of Physics and Astronomy, East Tennesse State University,Johnson City, TN 37614

ABSTRACT

Collisions of binary winds lead to a bow shock around the star that has a weaker wind. In the large scale, the weaker wind is confined into a spiral pattern as a function of time with orbital phase. We use a model for the shape of the confined companion wind to compute line profiles as a function of the physical parameters of the system. Our model is designed to be flexible to explore the orbital effects and shock properties, which will enable us to better understand the geometries, viewing inclinations, and wind properties of massive binary systems.

Subject headings: line: profiles—binaries: general—stars: Wolf-Rayet—stars: wind,outflows

1. INTRODUCTION

A stellar wind is a mass-loss flow of gas from the upper atmosphere of a star (Lamers & Cassinelli 1999). Especially interesting are two star systems which create an environment for the collision of winds. A binary system which includes a Wolf-Rayet star is optimal when trying to observe the effects of stellar wind collisions owing to its high mass-loss rate and high wind speed. Typical companion stars are massive O and B stars with somewhat lower mass loss rates but comparable wind speeds.

Wolf-Rayet (WR) stars are the evolved states of massive O stars and typically have from 10–25 $M_\odot$. With stellar wind speeds ranging from 1000-3000 km s^{-1}, a WR star loses around $10^{-5} M_\odot yr^{-1}$. The stars show broad emission lines of He with subclasses for N-rich types and C-rich types (Crowther 2007). WR stars represent the terminal stages of massive star evolution which expire in supernova explosions.

2. MODEL

We explored two cases of models to help understand the connection between observed Doppler broadened line shapes and the structure of colliding winds. In the first model, one visualizes cavity and compression zones as purely conical in shape and stationary. The second model includes the effects of orbital motion. We treat the confined wind of the companion star as the "cavity" in the sense that the forbidden lines being studied form in the WR wind. The compression zone is a zone of enhanced density that contains the shocked WR wind because of the wind collision. Our first model for a purely conical interaction region between the winds approximates long period binaries, whereas inclusion of orbital motion in the second model leads to a spiral morphology for the wind collision interface.

Our goal is to compute forbidden emission line profile shapes for colliding wind systems. Critical for understanding the effects is to know the relation between the spatial distribution of emission in the wind and the construction of line profiles. It is useful to think of the wind

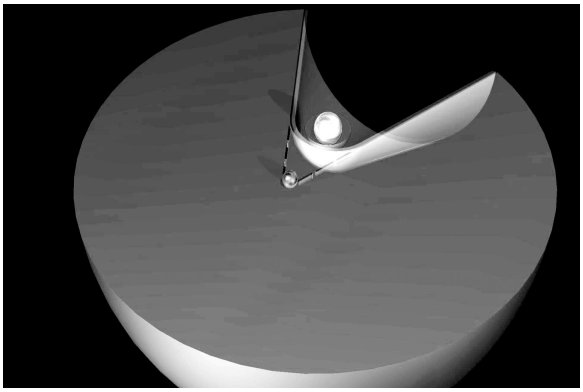

Fig. 1.— The Figure shows a cross-section of a spherical wind with the binary system and cavity/compression zones. (Image created by Nick Adams)

in terms of "cuts" known as "isovelocity zones". Isovelocity zones are surfaces where projected wind speeds with respect to a fixed observer are equal. Because forbidden lines form at a large radius, we adopt a wind model for the WR star that has constant radial expansion at the wind terminal speed v_∞. The line-of-sight Doppler shift toward the observer at any point in this spherical flow is

$$v_z = -v_\infty \cos\theta, \tag{1}$$

where θ is the spherical polar angle of the wind flow vector relative to the observer axis. We introduce a normalized velocity shift:

$$w_z = \frac{v_z}{v_\infty}. \tag{2}$$

Surfaces with constant w_z are surfaces of constant θ, and thus cones. These cones have their vertex at the WR star.

It is well-known that for an optically thin line (the case for forbidden lines) formed in a constant expansion and spherically symmetric wind, the resulting line shape is rectangular or "flat-topped", with equal emission per unit velocity shift from $-v_\infty$ to $+v_\infty$. The consequence of the wind collision will be to produce deviations from the flat-top shape. Such deviations are seen in forbidden lines of WR colliding wind binary systems (e.g., Ignace et

[1]Southeastern Association for Research in Astronomy (SARA) NSF-REU Summer Intern (2008)
Electronic address: zcsp12@goldmail.etsu.edu, ignace@etsu.edu

al. 2001). The introduction of a cavity and a compressed layer in the otherwise spherically symmetric wind of the WR star will modify the the spectral line shape (or leave a "footprint") that depends on the orbital and wind parameters, such as the shock opening angle β, the viewing inclination of the orbit i, the binary separation a, and mass-loss rates and terminal speeds of the two winds.

To understand the line profile shapes that come from colliding wind systems, it is important to understand first the line formation process. We adopt the two-level atom approximation for a fine-structure transition, following the notation of of Ignace & Brimeyer (2006). The upper level is assumed to be populated by collisional excitation only, whereas the lower level population is determined by collisions and decay from the upper level. One can define a critical density n_c to characterize where in the wind the de-excitations are dominated by collisions (high density) or decays (low density), as given by

$$n_c = \frac{A_{21}}{q_{21}}, \tag{3}$$

where A_{21} is the Einstein A-value in Hertz, and q_{21} is the volume rate of collisional de-excitations in units of cm^3-Hz.

The emissivity j_ν (erg s^{-1} cm^{-3} sr^{-1}) is given by

$$j_\nu = \frac{1}{4\pi}\, h\nu\ A_{21}\ n_2, \tag{4}$$

where h is Planck's constant and n_2 is the second level population density. This upper level population transitions from a linear function of the wind density at inner radii to a quadratic in density at large radii. Given that the density scales as r^{-2}, we can define a characteristic location in the wind where this change occurs, called the critical radius and given by

$$\frac{r_c}{R_\star} = \sqrt{\frac{n_0}{n_c}}. \tag{5}$$

Then the level two population becomes

$$n_2 = \frac{n_e}{(1+\omega) + (\omega\ R_\star^2/r_c^2)}, \tag{6}$$

where ω is a parameter that depends on the line transition (see Ignace & Brimeyer 2006).

It is also instructive to consider the total flux of line emission F_l (erg s^{-1} cm^{-2}) for the forbidden line. For an optically thin line, the flux is given by (Mihalas 1978)

$$F = \frac{1}{D^2}\int_{R_\star}^{\infty} j(r) dV. \tag{7}$$

Using a change of variable $u = R_\star/r$, the integral relation becomes

$$F_l \approx n_0 \int_0^1 \frac{du}{(1+\omega)u^2 + \omega {u_c}^2}. \tag{8}$$

For a spherical wind, this integral has an analytic solution F_s given by

$$F_s = n_0 \frac{1/u_c}{\sqrt{\omega(1+\omega)}} \arctan \sqrt{\frac{\omega}{1+\omega}} \left(\frac{u}{u_c}\right)\Bigg|_0^1. \tag{9}$$

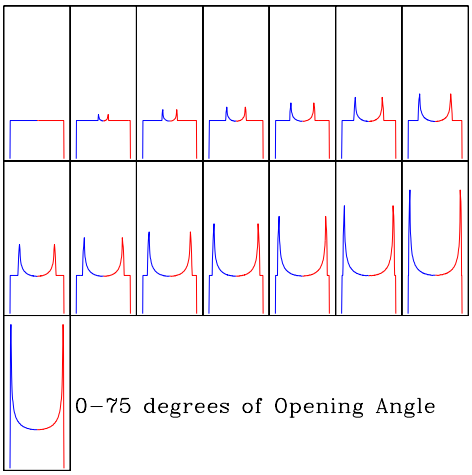

FIG. 2.— This plot has a fixed viewing perspective where the cavity/compression is at a 90 degree angle from the observer while the opening angle β grows by 5° increments.

Since $u_c \ll 1$, the arctangent factor reduces simply to $\pi/2$.

For the colliding wind system, one only has to omit emission from the cavity region. That part of the model was considered by Bessey & Ignace (2007). Here we also need to account for the compression layer. To do so, we require an estimate for the volume extent of the layer and its density structure. We assume the layer has a uniform density of four times the value in the spherical portion of the WR wind. Using mass continuity, it follows that the solid angle of the compressed zone will be one quarter that of the cavity zone. To estimate the influence of the compression layer for the line emission, consider what would happen to the total line flux for a spherical wind that is four times as dense. Using the preceding equations, one has that $n_0 \rightarrow 4n_0$, now giving

$$F_l \approx (4n_0)\ \frac{1}{\sqrt{\omega(1+\omega)}} \left(\frac{1}{u_c/2}\right)\ (\pi/2)\ = 8F_s \tag{10}$$

Since a spherical wind produces a flat-top profile, we conclude that the compressed zone will have 8 times the flux of the spherical portion per unit solid angle. Given that the compressed layer spans a quarter of the solid angle of the cavity in the form of a sheath-like boundary layer of the cavity, distinctive double-peaked profile contributions result that grow in both amplitude and separation as β increases. Emission from the compressed layer exceeds what is lost from the cavity region resulting in a net factor of two gain in line emission from a spherical equivalent. The fact that the net is not a zero sum game arises because the emissivity has a density-squared dependence at large radius. Note however that the actual amount of enhanced emission for our simulated lines will depend on (a) the binary separation, since the wind collision exists mostly beyond that radius and is spherical interior to it and (b) the opening angle of the shock because that sets the relative amount of the wind involved in the collision compared to the fraction that is treated as spherical.

3. RESULTS

Figure 2 shows a sequence of model lines as a function of the opening angle β of the cavity. The wind interaction is for the long period approximation, so the interaction region is conical. The viewing inclination is set at $i = 90°$, meaning that the cone axis lies in the plane of the sky, hence the emission profiles are symmetric about line center. A distinctive double-peaked profile results, growing in both amplitude and separation as β increases.

Figure 3 shows a different case. Here $\beta = 50°$ is fixed, and i of the conical interaction region is allowed to change. Upper left shows the case for nearly looking down the cone axis. Deviations from flat-top are entirely blueshifted. Moving rightward, the i increases to 90°, where the profile is seen as symmetric. Repeating this at the lower far right and moving leftward shows increasing inclinations until the cone is nearly directly away from the observer as in the last panel at lower left.

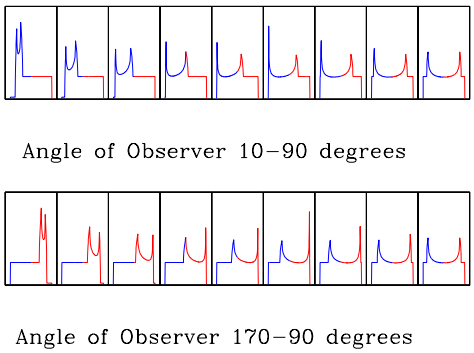

FIG. 3.— This plots shows the effect of changing viewing angle inclination i from 10–170 degrees with a fixed opening angle β of the cavity/compression of 50 degrees.

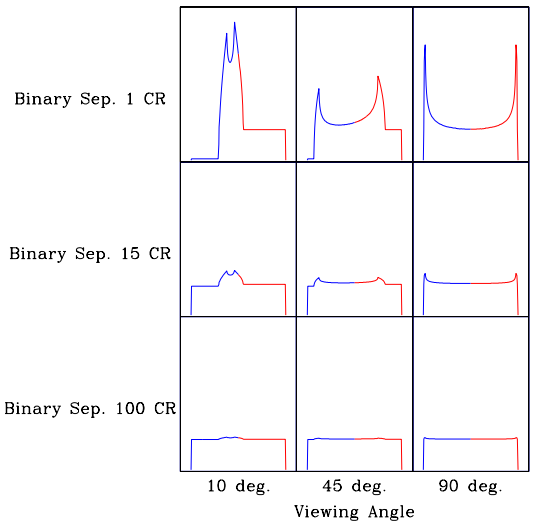

FIG. 4.— This plot shows a trend of increasing binary separation in terms of critical radii with 3 different viewing perspectives

Figure 4 shows the influence of binary separation, with i indicated. The binary separation is given in terms of the critical radius. We expect that as the binary widens for a r_c fixed, the effects of the colliding wind interaction will diminish, which is confirmed. However, it is somewhat surprising still to see significant deviations from flat-top at $15r_c$. This occurs because the flux in the compression layer is sensitive to the square of the wind density for the outer wind.

4. CONCLUSIONS

When considering the collisions of stellar winds, there are many parameters that influence the shape of emission line profiles. We focused on a conical bow shock with both the absence of emission in a confined companion wind (cavity) and an enhancement of emission in a shocked layer (compression) that jackets the cavity region. In the conical model, there are features in the line profiles that can be related directly to physical properties of the system and stars.

In the future, line profiles that account for the companion orbiting the WR star will be calculated. As illustrated in Figure 5, the radial extent of the cavity/compression portion is different with orbital phase. This results from Kepler's second law for an eccentric orbit given that the WR wind speed is constant with phase. For a circular orbit, there will be no phase dependence to the appearance of the spiral.

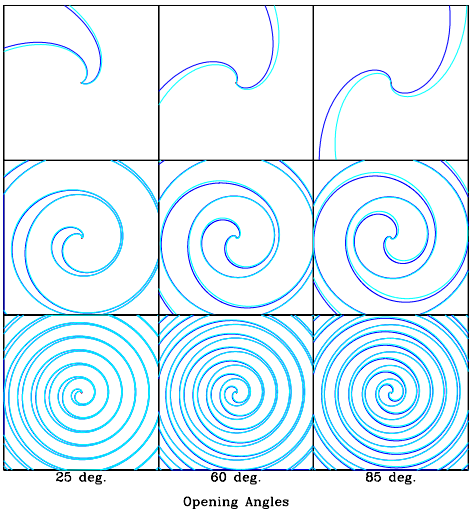

FIG. 5.— This plot shows different opening half-angles β of the cavity/compression and then zooms out to reveal a top view of the projected spiral path in the orbit plane. The eccentricity of the orbit is fixed at 0.5.

This project was funded by a partnership between the National Science Foundation (NSF AST-0552798), Research Experiences for Undergraduates (REU), and the Department of Defense (DoD) ASSURE (Awards to Stimulate and Support Undergraduate Research Experiences) programs.

REFERENCES

Barlow, M. J., Roche, P. F., & Aitken, D. K. 1988, MNRAS, 232, 821
Bessey, R., & Ignace, R. 2007, JSARA, 1, 28
de Marco, O., et al. 2000, A&A, 358, 187
Dessart L., Crowther P. A., Hillier D., Willis A. J., Morris P. W., & van der Hucht K. A. 2000, MNRAS, 315, 407
Ignace R., Cassinelli J. P., Quigley M., & Babler B. 2001, ApJ, 558, 771
Ignace, R., & Brimeyer, A. 2006, MNRAS, 371, 343
Ignace, R., Cassinelli, J. P., Tracy, G., Churchwell, E. 2007, ApJ, 669, 600
Lamers H. J. G. L. M., Cassinelli J.P. 1999, Introduction to Stellar Winds, New York, Cambridge University Press
Mihalas, D., 1978, Stellar Atmospheres, 2nd ed., (New York: W. H. Freeman and Company)
Morris P. W., van der Hucht K. A., Crowther P. A., Hillier D. J., Dessart L., Williams P. M., & Willis A. J. 2000, A&A, 353, 624
Smith J. R. 2005, ApJ, 622, 1044
Stevens, I. R., Blondin, J. M., Pollock, A. M. T. 1992, ApJ, 386, 265
Walder, R. 1998, Ap&SS, 260, 243